THE JOURNAL OF BIOLOGICAL CHEMISTRY
Vol. 266, No. 11, Issue of April 15, pp. 6957-6965, 1991
Printed in U.S.A.

Assay of Metabolic Superoxide Production in *Escherichia coli**

(Received for publication, September 26, 1990)

James A. Imlay‡ and Irwin Fridovich§

From the Department of Biochemistry, Duke University Medical Center, Durham, North Carolina 27710

Superoxide production has been measured in subcellular fractions of SOD-deficient *Escherichia coli* provided with physiological reductants. Although cytosolic enzyme(s) do generate O_2^-, the larger portion is produced by autoxidation of components of the respiratory electron-transport chain. At 37 °C and with pO_2, NADH, and NAD^+ levels matching those *in vivo*, respiring membrane vesicles generate 3 O_2^-/10,000 electrons transferred. This corresponds to intracellular O_2^- production, in glucose-fed cells, of 5 μM/s. The high SOD content of normal cells restricts O_2^- accumulation to $2 \cdot 10^{-10}$ M, with a moderate gradient from the membrane to the center of the cell. SOD-deficient mutants achieve a much higher steady-state content of O_2^-. Rates of superoxide-mediated inactivation of certain enzymes are sufficiently rapid that even 10^{-10} M O_2^- imposes a significant oxidative stress.

Molecular oxygen is potentially a powerful chemical oxidant. The survival of carbon-based life in an aerobic environment is possible only because a spin restriction kinetically impedes the multivalent reduction of oxygen (1). However, univalent electron transfer to molecular oxygen is facile, resulting in the genesis of the superoxide radical. The virtual ubiquity in aerobic organisms of superoxide dismutases (SOD)[1] indicates that O_2^- generation can occur at a rate which would be toxic in the absence of defensive enzymes. Indeed, SOD-deficient mutants of *Escherichia coli*, yeast, and *Drosophila* have been isolated, and all exhibit severe oxygen-dependent growth impairments (2–5). It has been proposed that sufficient O_2^- eludes the scavenging systems in SOD-proficient organisms to impart a chronic oxidative stress that leads to senescence (6, 7).

Because O_2^- is modestly reactive as either oxidant or reductant, it is selective in its targets, and the identities of critically vulnerable biomolecules are only partially known. Mutants of *E. coli* devoid of SOD mutate spontaneously at a high rate (8); this is thought to ensue from the participation of O_2^- in a Haber-Weiss reaction, producing a strong mutagen such as $HO\cdot$ or FeO^{2+}. These strains also suffer from deficiencies in the biosyntheses of branched-chain, aromatic, and sulfur-containing amino acids (4), presumably due to superoxide-mediated damage to biosynthetic enzymes. O_2^- inactivates the dihydroxyacid dehydratase of branched-chain amino acid biosynthesis by attacking its active-site iron-sulfur cluster (9, 10), and a similar mechanism may account for the superoxide sensitivity of the 6-phosphogluconate dehydratase of the Entner-Doudoroff pathway (11).

As additional targets for attack by O_2^- are revealed, it becomes increasingly important to estimate the oxidative stress to which they are exposed *in vivo*. This entails a determination of the steady-state O_2^- concentration in growing cells. Estimates of 10^{-12}–10^{-11} M have been made for rat liver mitochondria, based on the rate of hydrogen peroxide evolution (12); but, as the author notes, this calculation is subject to error due to the use of optimal substrate and ADP concentrations and nonphysiological pO_2.

We have measured O_2^- production by subcellular fractions of SOD-deficient *E. coli*. The major site of O_2^- generation is the respiratory chain of the cell membrane. By determining the O_2^- flux as a fraction of respiratory electrons transferred, we are able to estimate the rate of O_2^- production within the growing cell. This information, coupled with measurements of intracellular SOD activity, permits calculation of steady-state O_2^- concentrations in growing *E. coli*.

EXPERIMENTAL PROCEDURES

Strains—AB1157 (F⁻ *thr-1 leuB6 proA2 his-4 thi-1 argE2 lacY1 galK2 rpsL supE44 ara-14 xyl-15 mtl-1 tsx-33*) and JI132 (as AB1157 plus (*sodA*::Mu d PR13)25 (*sodB-kan*) 1-Δ2) were obtained from Stuart Linn (13). IY13 (F⁻ *thi his ilv trp rpsL*) and IY12 (as IY13 plus *ndh*) were provided by Ian Young (14).

Horse heart ferricytochrome *c* (type III), *E. coli* MnSOD, yeast alcohol dehydrogenase, succinic acid, α-glycerolphosphate (grade X), L-lactic acid, D-lactic acid, flavin mononucleotide, *Vibrio fischeri* luciferase, L-glutamic dehydrogenase ($NADP^+$), NAD^+, NADH, and NADPH were from Sigma. Bovine erythrocyte Cu,ZnSOD was a gift of Leopold Flohé, Grunenthal GMBH, Stolberg, Germany. [U-^{14}C] sucrose was from Amersham Corp. Tritiated water and xanthine oxidase were kindly provided by K. V. Rajagopalan. Formic acid and potassium cyanide were purchased from the J. T. Baker Chemical Company.

Cell Growth and Preparation of Extracts—For the preparation of extracts, cells were grown in glucose-supplemented LB medium (10 g of bactotryptone, 5 g of yeast extract, 10 g of NaCl, 2 g of glucose, per liter, pH 7.0), minimal A medium (15) containing 2 g/liter glucose and 60 μg/ml of the necessary L-amino acids, or casamino acids medium (as minimal A medium, but with 1% casamino acids replacing glucose). Cells were cultured for at least five generations in flasks at 37 °C with vigorous shaking and were harvested at 0.3–0.6 OD_{600}. Cultures were centrifuged, washed in cold 50 mM potassium phosphate buffer, pH 7.8, and resuspended to about 3% of the original volume in this phosphate buffer. Optical density was determined immediately prior to lysis. (The relation between optical density and cell number was determined with the strains, media, and cell densities used in this study by counting cells in a Petroff-Hauser bacteria counter under a light microscope.) The cell suspension was then passed through a French pressure cell at 20,000 p. s. i. and centrifuged for 20 min at 13,000 × *g* to remove cell debris. Lysis was essentially complete, as manifested by loss of turbidity and by cell mortality.

* This work was supported in part by grants (to I. F.) from The Council for Tobacco Research, Inc., the American Cancer Society, the National Science Foundation, and the National Institutes of Health. The costs of publication of this article were defrayed in part by the payment of page charges. This article must therefore be hereby marked "*advertisement*" in accordance with 18 U.S.C. Section 1734 solely to indicate this fact.

‡ Fellow of the Jane Coffin Childs Memorial Fund for Medical Research.

§ To whom correspondence should be addressed: Dept. of Biochemistry, Duke University Medical Ctr., Durham, NC 27710. Tel.: 919-684-5122.

[1] The abbreviations used are: SOD, superoxide dismutase; LB, Luria broth.

The supernatant, which contained both cytosolic material and membrane vesicles, was fractionated by a 3-h centrifugation at 85,000 × *g*. The supernatant cytosol fraction was removed and the pelleted membrane vesicles were resuspended in phosphate buffer by vigorous pipetting, and both fractions were recentrifuged. The final vesicle suspension was in 0.2% of the original culture volume and contained at least 95% of the NADH oxidase activity remaining after removal of the cell debris from the homogenate. Vesicles prepared in this manner are inverted (16) and will oxidize respiratory substrates and reduce O_2 on their external face. The vesicles exhibited apparent K_m values for NADH and O_2 of about 15 and 1.5 μM, respectively, at 37 °C. The stoichiometry of NADH:O_2 consumed was 2:1. No measurable SOD activity was present in the vesicle fractions of SOD-proficient cells. Both cytosolic and vesicle fractions were stored at 0 °C; less than 10% of the O_2^- production and respiratory activities were lost during 1 week of storage. Protein content was determined by the Bradford dye-binding assay (17).

Detection of O_2^-—O_2^- formation was measured as SOD-sensitive cytochrome *c* reduction. Cytochrome *c* oxidase activity, which interferes with this assay in mammalian mitochondria, was absent from the *E. coli* extracts. Respiratory vesicles and cytosolic fractions were assayed in slightly different ways. Cytosolic fractions were assayed in 3-ml reaction volumes containing 20 μM cytochrome *c*, NADH, NAD^+, or other reactants as indicated, and cytosolic extract in 50 mM phosphate buffer (pH 7.8). Duplicate reactions were performed, one of which contained 20 units of SOD. The extent of cytochrome *c* reduction was checked intermittently at 550 nm and expressed in terms of concentration using the relation $\epsilon_{mM}\ cyc^{2+} - \epsilon_{mM}\ cyc^{3+} = 21.0$. Periodic illumination with 550-nm light had no effect on cytochrome *c* reduction. Substrate stock solutions were adjusted to pH 7.8 prior to use. Unless otherwise indicated, reactions were at 37 °C.

Preliminary measurements of O_2^- production by membrane vesicles were conducted at room temperature in 3-ml reaction volumes containing 10 μM cytochrome *c*, respiratory substrates (300 μM NADH, 20 mM succinate, 20 mM formate, 1 mM L-lactate, 20 mM D-lactate, or 20 mM α-glycerolphosphate, all at pH 7.8), and membranes. The membrane content was sufficiently low that <50% of the dissolved oxygen was consumed during the period of observation. When used, KCN was adjusted to pH 7.8 and added to a final concentration of 1.0 mM.

In experiments designed to simultaneously measure O_2^- production and respiration at 37 °C, alcohol dehydrogenase and ethanol were added to recycle NAD^+, and reactions were carried out in well shaken flasks to prevent depletion of oxygen. Reaction mixtures were divided into three aliquots to allow monitoring of 1) NADH content and respiration rate, 2) total cytochrome *c* reduction, and 3) SOD-resistant cytochrome *c* reduction. For example, 50 ml of KP_i (pH 7.8, 37 °C) was warmed in a 125-ml flask (A) with 2 mM NAD^+, 0.76% ethanol, and 75 units alcohol dehydrogenase, and membranes were added to start the reaction. Sixteen ml were immediately removed to a 50-ml flask (B) containing 0.48 μmol of cytochrome *c*, and 8 ml was moved from flask B into a third flask (C) containing 50 units of MnSOD. At intervals, 1-ml aliquots were removed from flask A into a thermostatted spectrophotometer to monitor the degree of NAD (H) reduction at 340 nm. (Failure to thermostat the spectrophotometer will result in a displacement of the NADH/NAD^+ equilibrium from that pertaining at 37 °C.) In some cases, aliquots (2.5 ml) were also removed from flask A to a Clarke electrode at 37 °C to monitor oxygen consumption. Aliquots from flasks B and C were examined intermittently to monitor total and SOD-resistant cytochrome *c* reduction, respectively. Because acetaldehyde gradually accumulates and displaces the alcohol dehydrogenase equilibrium, the NADH/NAD^+ ratio slowly declines, affecting both the rates of respiration and of O_2^- production. (The competitive inhibition of NADH binding by NAD^+ raises the apparent K_m to 30 μM, and ethanol has a modest additional effect, so that some experimental NADH concentrations were sub-saturating.) The period of observation was divided into 5- to 10-min intervals during which the mean O_2 consumption rate, O_2^- production rate, and NADH content were correlated. Discounting the minor affects of changes in NADH concentration, the rates of oxygen consumption and superoxide production were stable throughout a 2-h incubation period. The action of alcohol dehydrogenase alone produced no detectable O_2^-. Correction was made for a small background of membrane-independent O_2^- production, which was directly proportional to [NADH] and probably due to autoxidation. In some cases, rather than measure O_2 consumption, a parallel reaction omitting alcohol dehydrogenase and with a lower membrane content was monitored at 340 nm to determine the dependence of NADH oxidation on [NADH] at a given ethanol concentration.

SOD Assays—Superoxide dismutase was assayed using the xanthine oxidase/cytochrome *c* method (18).

Cell Size—The size of AB1157 was determined by measuring the water-accessible sucrose-excluding volume of a pellet containing a defined number of cells. Cells were grown exponentially in the indicated medium to $OD_{600} \approx 0.4$, chilled, centrifuged, and resuspended in 20 ml of the same cold medium. Some of the cell-free supernatant (S1) was reserved for later use. A small aliquot of the cell suspension was removed and diluted, and its optical density was determined at 600 nm. A solution containing 1.4 mCi of [^{3}H]H_2O and 0.12 mCi of [U-^{14}C]sucrose in 0.25 ml of 230 mM sucrose was prepared. We added 0.1 ml of this solution to the 20-ml cell suspension. The cells were maintained on ice for 5 h and then recentrifuged at 12,000 × *g* × 10 min. The radioactive supernatant (S2) was put aside, and the pellet (P2) was resuspended in 10 ml of the unlabeled cold (S1) supernatant. After 5 h, the cells were recentrifuged and the supernatant (S3) was saved. Fraction S2 represents the radioisotope mix to which the cells were exposed, and fraction S3 represents the radioactivity carried down with the cells. This pelleted radioactivity includes that from the interstitial fluid within the cell pellet as well as that from the intracellular volume. The activity of tritium in the pellet (P2) matches that of the supernatant (S2), so that the pellet volume P2 can be calculated as follows.

$$\text{Volume of P2} = \frac{\text{total } ^3\text{H in S3}}{\text{total } ^3\text{H in S2}} \times \text{(volume of S2)}$$

Similarly, the interstitial pellet volume can be calculated as follows.

$$\text{Interstitial volume of P2} = \frac{\text{total } ^{14}\text{C in S3}}{\text{total } ^{14}\text{C in S2}} \times \text{(volume of S2)}$$

Finally, the intracellular solvent volume can be obtained by subtraction as follows.

$$\text{Intracellular volume} = \text{total volume} - \text{interstitial volume}$$

During scintillation counting the windows were adjusted to minimize the overlap of the ^{3}H and ^{14}C energy profiles, and the automatic quench compensation routine that is built into the Beckman LS1801 scintillation counter was activated. The degree of residual overlap in high- and low-energy windows was determined by counting separate single-label samples of [^{3}H]H_2O and [U-^{14}C]sucrose in supernatant S1. By solving the simultaneous equations for ^{3}H and ^{14}C distributions between the high- and low-energy windows, the contributions of each could be determined in the measured samples. All scintillation samples were prepared in triplicate in Aquasol-2 scintillation fluid.

Determination of Intracellular Dinucleotide Pools—Methods for analysis of dinucleotide pool sizes were adapted from procedures described previously (19, 20). Bacteria were grown in 200-ml cultures in 1.0-liter flasks with vigorous shaking to $OD_{600} = 0.4$. For determination of total NAD(P)H and NAD^+, the culture was divided into two 100-ml portions; one was centrifuged, and its supernatant was retained for use in diluting standards. The optical density at 600 nm of the remaining 100-ml culture was determined, and it was then split into two 50-ml aliquots. The cell-free (sham) supernatant was also split, and its subsequent treatment was identical to that of the samples. To determine NAD(P)H, 2.5 ml of 2.5 M KOH was added to one 50-ml portion, which was then incubated 10 min at 50 °C and then neutralized to pH 7.0. The other 50-ml culture, intended for NAD^+ determination, was lysed by one passage through a French pressure cell, acidified with HCl to pH 2 to destroy NADH, incubated 10 min at room temperature, and then neutralized with KOH to pH 7.0. (Cell lysis by alkali or French press was performed immediately after the determination of optical density to ensure the correspondence between dinucleotide values and cell number. Furthermore, the cell cultures were agitated at 37 °C until the moment of lysis so that no anoxia- or cold-induced changes in redox status could occur. Centrifugation and washing steps, which are often included in NAD^+-determination protocols, were omitted because of the possibility of leakage of NAD(P)(H) during chilling (21). As a consequence, cells could not be concentrated prior to NAD(H) assay, and the growth medium, which can quench luminescence, was present in all samples.) The neutralized samples were centrifuged at 10,000 × *g* × 10 min to remove membrane fragments. The luciferase cocktail consisted of 10 mM KP_i (pH 7.0), 0.05% β-mercaptoethanol, 0.1 mg/ml decanal, and 0.2 mg/ml flavin mononucleotide. Various volumes of sample in the photometer tube were brought to a total volume of 2.4 ml by the

addition of the sham sample, and 0.3 ml of reaction mixture was added. For determination of NAD(P)H, 0.6 mg of luciferase was added to initiate the reaction, and the maximal amplitude of light emission was noted. For determination of NAD^+, about 50 units of alcohol dehydrogenase and 70 μl of 95% ethanol were included in the reaction mix before the addition of luciferase, and the steady-state level of light emission was recorded. Standard samples of NADH and NAD^+ were measured in sham extracts. Light responses were proportional to NAD^+ and NADH content in the 0.25–2.5 and 0.05–0.3 nmol ranges used in these assays. The use of sham treatments for standard solutions was absolutely necessary, since quenching of the light signal by the salty medium approached 90%. Surprisingly, the *Vibrio fischeri* luciferase, which contains an essential oxidoreductase as well as the true luciferase, was active with NADPH as well as NADH. In order to determine the concentration of each, the alkali-lysed culture was neutralized to pH 8.3 rather than 7.0, and α-ketoglutarate and NH_4Cl were added to final concentrations of 5 and 10 mM, respectively. The sample was split into four: to one (to measure NADH + NADPH), nothing was added; to a second (to measure NADH), $NADP^+$-specific glutamate dehydrogenase was added to a final activity of 0.3 units/ml; to a third (to measure NADPH), respiratory membranes prepared as described previously were added to a final activity of 0.5 units/ml of NADH oxidase; and to the fourth (blank), both glutamate dehydrogenase and respiratory membranes were added. The samples were incubated 10 min at room temperature. The pH was then adjusted to pH 12 with KOH and was then neutralized to pH 7.0 with HCl. Experiments with standard samples confirmed that the glutamate dehydrogenase eliminated signals due to NADPH, the membranes eliminated signals due to NADH, and in concert they reduced sample signals to zero. Both enzymes are absolutely specific for their cofactors. The final alkali/acid titration inactivated these enzymes and allowed NAD(P)H standards to be added back to the blank sample. Because the luciferase exhibits greater affinity for NADH than for NADPH, the photoemission maximum is slightly greater for NADH, and so NADH standards were employed for determinations of NADH and NADPH standards for determinations of NADPH. NADH and NADPH concentrations in stock solutions were determined by their absorbance at 340 nm ($\epsilon_{mM} = 6.2$).

RESULTS

Detection of Superoxide Production by NADH-treated Fractions—In preliminary experiments, cytoplasmic or membrane fractions of *E. coli*, in the presence of NADH, slowly reduced cytochrome *c* (Fig. 1). With either fraction the addition of superoxide dismutase inhibited the rate of cytochrome *c* reduction by 30–50%. Excessive quantities of SOD did not further lessen the rate of cytochrome *c* reduction, and the SOD-sensitive portion exhibited the competitive kinetics between SOD and cytochrome *c* to be expected from their relative reaction rates with O_2^- (data not shown). The MnSOD from *E. coli* and the Cu,ZnSOD from bovine erythrocytes were equally effective on a per-unit basis, whereas heat-inactivated manganese SOD was not inhibitory (data not shown). Collectively, these data indicate that a part of the cytochrome *c* reduction was mediated by O_2^-. O_2^- production was absolutely dependent upon the presence of NADH and was proportional to the concentration of either cytoplasmic or membrane fractions.

Localization of the Sites of O_2^- Production—The identity of the cytoplasmic O_2^- source has not been established. NAD^+ was an inhibitor of NADH-dependent O_2^- production at 25 °C, reducing the O_2^- flux by 50% at ~25 μM NAD^+ and almost entirely at the millimolar concentrations found in the cell (Fig. 2). The inhibition was not competitive. Because the inhibition was monophasic, the cytosolic O_2^- production may be due to a single enzyme. NADPH also stimulated the cytoplasm to make O_2^-, although at a slightly lower rate than did NADH. Since the addition of NADPH did not further increase O_2^- generation by an NADH-treated extract, these two reduced dinucleotides probably compete to reduce the same O_2^--generating enzyme(s) (Table I).

Inverted membrane vesicles were used so that externally

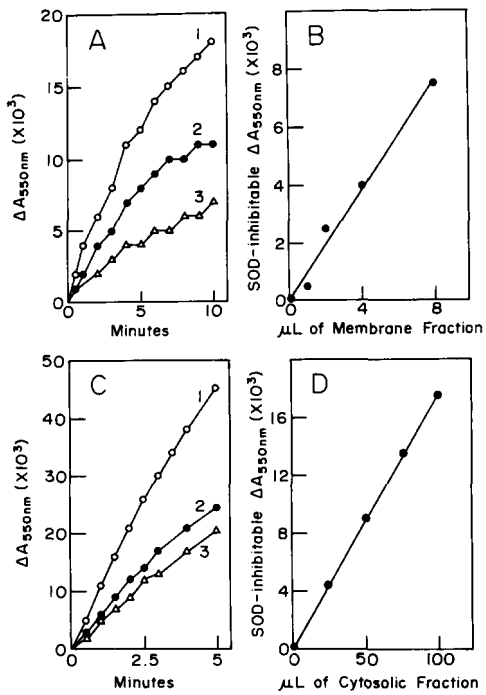

FIG. 1. **Superoxide production by NADH-treated cell extracts.** *A*, time course of cytochrome *c* reduction by membrane vesicles. Vesicles (4 μl, 37 units/ml NADH oxidase), NADH (300 μM), and cytochrome *c* were incubated at 22 °C with or without SOD. *Curve 1*, total cytochrome *c* reduction; *curve 2*, SOD-resistant cytochrome *c* reduction; *curve 3*, O_2^--dependent cytochrome *c* reduction (obtained by subtraction). *B*, superoxide production *versus* membrane concentration. Net SOD-sensitive cytochrome *c* reduction was determined after 5 min. *C*, time course of cytochrome *c* reduction by the NADH-treated cytosolic fraction of an SOD-deficient mutant. Cytosol (50 μl, 2.9 mg protein/ml), NADH (300 μM), and cytochrome *c* were incubated at 22 °C with or without SOD. *Curve 1*, total cytochrome *c* reduction; *curve 2*, SOD-resistant cytochrome *c* reduction; *curve 3*, SOD-sensitive cytochrome *c* reduction. *D*, superoxide production *versus* volume of cytosolic extract containing 2.3 mg protein/ml. Net SOD-sensitive cytochrome *c* reduction was determined over 4 min.

applied reductants could drive the respiratory pathway. The O_2^- measured in the suspending medium would normally have been produced on the cytoplasmic face of the membranes of intact cells. O_2^- was not generated upon incubation of membranes with NADPH, consistent with the specificity of the respiratory NADH dehydrogenase (Table II). Cyanide inhibited respiratory function and amplified O_2^- formation, suggestive of electron leakage from a respiratory component upstream of the cyanide-sensitive cytochrome oxidase. Membrane vesicles prepared from a strain that lacks the respiratory NADH dehydrogenase failed to generate O_2^- upon incubation with NADH. Thus a member of the respiratory pathway was clearly the site of O_2^- production on the vesicles.

Intracellular Dinucleotide Concentrations—In order to mimic intracellular O_2^- production with cell extracts and membrane vesicles, it is important to establish substrate conditions similar to those in the cell. The NADH and NAD^+ contents of log-phase cells were determined after growth in LB medium and in a minimal salts medium (Table III). Cells were lysed by the direct addition of alkali without any intermediate centrifugation steps, to ensure that the redox status of the cell was not perturbed by chilling or exhaustion of oxygen. Some variability was observed from preparation to preparation. This was expected, since the cells upon harvesting (~$1:10^8$ cells/ml) were in the midst of metabolic transition as the glucose content of the medium declines. The NAD(H)

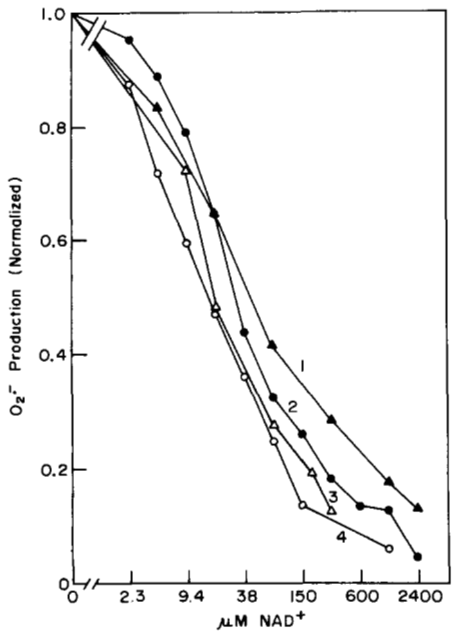

FIG. 2. **Cytosolic O_2^- production by NADH is inhibited by NAD+.** Activities have been normalized to those observed in the absence of NAD^+, *i.e.* 3.6, 3.4, 3.2, and 2.4 nmol of O_2^-/min/mg of protein, respectively, when NADH was present at 300 (*curve 1*), 75 (*curve 2*), 19 (*curve 3*), and 4.7 (*curve 4*) μM.

TABLE I

O_2^- Formation by cytosolic enzymes

The cytosolic fraction was prepared from the SOD-deficient strain JI132 after growth in LB medium, and O_2^- formation was measured at 25 °C as described under "Materials and Methods." Reduced dinucleotides were present at 300 μM and KCN at 1 mM.

	O_2^-/min-mg protein
	nmol
NADH	3.9
NADPH	2.5
NADH + NADPH	3.8
NADH + KCN	3.9

TABLE II

O_2^- Formation by membrane vesicles

IY13 (*ndh*+) and IY14 (*ndh*−) were grown to log phase ($OD_{600\ nm}$ = 0.4) in LB medium, and membrane vesicles were prepared and assayed for O_2^- production. Reduced dinucleotides were present at 300 μM and KCN at 1 mM. O_2^- production rates were normalized to that of *ndh*+ vesicles incubated with NADH: 0.08 μM O_2^-/min with 0.1 mg/ml protein in the test solution.

	Activity	
	ndh+	*ndh*−
	%	
NADH	100	<8
NADPH	<8	
NADH + KCN	380	<8
NADPH + KCN	<8	

pool was predominantly oxidized, and [NADPH] invariably exceeded [NADH].

Cell volumes were determined in order to convert the dinucleotide content into intracellular concentrations. The concentrations were similar for cells grown in rich and minimal glucose-containing media. [NADH] amply exceeded the K_m of the NADH dehydrogenase.

Intracellular Oxygen Concentration—The amplification of O_2^- production by the addition of cyanide to membrane vesicles indicates that electron donation to O_2 occurs at a site other than the oxygen-binding site of the cytochrome oxidase. Thus O_2 intercepts the respiratory electrons at a position that has not evolved to bind oxygen and which probably would not exhibit saturation with O_2. It is likely, then, that O_2^- production would increase in proportion to $[O_2]$ within the cells. (A first-order relation between dissolved O_2 concentration and O_2^- production has been reported for mitochondrial membranes (22, 23); a similar relation was suggested but not rigorously established by the experiments with membrane vesicles reported herein.) O_2 is more soluble in nonpolar solvents than in water, making it unlikely that the cell membrane constitutes a barrier to its entry into the cell.

TABLE III

Cell parameters of log-phase AB1157

	LB	Minimal salts
NAD^+ concentration (mM)	1.8	2.6
NADH concentration (μM)	70–200[a]	100
NADPH concentration (μM)	190–600[a]	180
Cell volume (liters)	$3.2 \cdot 10^{-15}$	$6.8 \cdot 10^{-16}$
SOD activity (units/ml internal volume)	3600	2400
Respiration (molecules O_2/cell/s)	$6.2 \cdot 10^6$	$9.0 \cdot 10^5$

[a] Range of values from four preparations.

Our analysis of the data of Kita *et al.* (24) confirms that the intracellular and extracellular oxygen concentrations are very similar. In the steady state, oxygen flux and consumption are balanced. For this diffusive process, the rate of influx is proportional to the oxygen gradient, whereas the consumption exhibits Michaelis-Menten behavior

$$D([O_2]_{out} - [O_2]_{in}) = V_{max}\left(\frac{[O_2]_{in}}{K_m + [O_2]_{in}}\right)$$

where D is the diffusion coefficient, $[O_2]_{out}$ and $[O_2]_{in}$ represent solution and intracellular oxygen concentrations, respectively, and V_{max} is the maximum velocity of the cytochrome oxidase. Kita *et al.* (24) determined an apparent K_m for respiratory oxygen reduction of 1.8 μM O_2 with intact log-phase cells and 1.4 μM O_2 with inverted vesicles. Thus at 1.8 μM external O_2, the internal O_2 was 1.4 μM, since 1.8 μM external O_2 gave the same degree of oxidase function inside whole cells as did 1.4 μM with inverted membranes.

$$D(1.8_{out} - 1.4_{in}) = V_{max}(0.5)$$

$$V_{max} = 0.8D$$

Then at the external O_2 concentration of 210 μM that is found in growth medium at 37 °C, which is equilibrated with air,

$$D(210_{\mu M} - [O_2]_{in}) = 0.8D\left(\frac{[O_2]_{in}}{1.4 + [O_2]_{in}}\right)$$

$$(210 - [O_2]_{in})\ (1.4 + [O_2]_{in}) = 0.8[O_2]_{in}$$

which solves to the quadratic $[O_2]_{in}^2 - 207.8\ [O_2]_{in} - 294 = 0$. The solution is $[O_2]_{in} = 209.2$. Thus the oxygen gradient across the cell membrane is negligible. Similar analysis of their data from stationary-phase cells, which contain a kinetically distinct cytochrome oxidase, indicates an internal O_2 concentration of 209.9 μM when the external concentration is 210 μM. Therefore the oxygen available to the inverted vesicles during our measurements of O_2^- production did not differ from that present inside intact cells.

Cell Volume—Cell volumes are indicated in Table III. Approximately 50% of the cell pellet was interstitial volume. The measurements represent solvent-accessible volume rather than the total volume occupied by an intact cell; since

about 30% of the total cell volume is solvent-excluding (24a), the distinction is significant.

Respiration—Respiration rates of log-phase cells were determined at 37 °C with a Clarke electrode (Table III). The respiration rate of *E. coli* is impressive; a single cell in aerated LB medium at 37 °C consumes six million molecules of oxygen/s. In the glucose-based minimal medium the rate was one-seventh as great, but this is due mainly to the difference in cell size. LB-grown cells consume an amount of oxygen equivalent to that dissolved within the cell eleven times per second; minimal medium-grown cells, seven times/s.

This large respiratory flux is almost entirely from oxidation of NADH. Log-phase cells grown in glucose-containing medium contain virtually no respiratory dehydrogenase activity for D- or L-lactate, succinate, α-glycerolphosphate, or formate (Table IV). By contrast, medium containing casamino acids as the sole carbon source causes a lower expression of NADH dehydrogenase activity and increased levels of the other dehydrogenases. These respiratory substrates stimulate O_2^- production by membranes at different rates per unit O_2 consumption, so it is not possible to predict total O_2^- production without knowledge of how much each dehydrogenase contributes to the total respiration.

SOD Content—The SOD activities of cell extracts were determined (Table III). Cells grown in rich medium have intracellular SOD activities of 3600 units/ml, in minimal medium, 2400 units/ml. Both the iron- and the manganese-containing SODs have specific activities of approximately 4500 units/mg and molecular weights of 46,000 and 42,000, respectively. One can then calculate that an LB-grown cell contains about 35,000 SOD molecules and a minimal-grown cell about 5000. (Again, this difference is largely due to the disparity in cell size.)

Respiratory O_2^- Production—It was desirable to measure O_2^- production at 37 °C with physiological substrate concentrations. Cyanide amplifies O_2^- production because it blocks electron outflow from the respiratory chain and thereby increases the degree of reduction of electron-chain components. Since the degree of reduction might also be modulated by NADH and NAD^+ ratios, it was important to control their concentrations while measuring O_2^- production. This was done by employing alcohol dehydrogenase (ADH) to recycle NAD^+ as follows.

$$NADH + \tfrac{1}{2}\,O_2 \xrightarrow{\text{membranes}} NAD^+ + H_2O \quad (1)$$

$$NAD^+ + \text{ethanol} \overset{\text{ADH}}{\rightleftharpoons} NADH + \text{acetaldehyde} \quad (2)$$

The equilibrium of Reaction 2 was adjusted by varying the amount of ethanol in the reaction. Ethanol did not alter the fraction of the electron flow converted to O_2^-. This is shown by the data in Fig. 3 which reflect results at ethanol concentrations ranging from 0.76 to 3.8%. Measurements in the absence of ethanol were difficult because depletion of NADH then occurred rather rapidly. Nevertheless, initial rate measurements indicated that the fractional O_2^- production was fully independent of the presence of ethanol (data not shown). Because acetaldehyde gradually accumulates and displaces the equilibrium, the consequent decline in NADH concentration was monitored during the reactions. This allowed O_2^- production rates to be determined at NADH concentrations between 30 and 275 μM. The data of Fig. 3 indicate that superoxide production is a constant fraction of respiratory rate over this range: 3.0–3.5 molecules of O_2^-/10,000 electrons transferred. Not surprisingly, changes in NAD^+ concentration were also without effect. Quantitatively consistent ratios of O_2^- production to respiration were obtained from nine independent membrane preparations prepared from four strains of *E. coli*. Membranes from SOD-deficient and SOD-proficient cells exhibited no differences. Furthermore, there was no significant difference in relative O_2^- production when the membranes were prepared from cells grown in minimal rather than LB medium.

Nonrespiratory O_2^- Production—O_2^- production from NAD(P)H by cytosolic enzymes was measured at 37 °C with extracts of the SOD-deficient strain JI132 (Fig. 4). (Measurements could not be made with extracts of cells grown on minimal medium since the SOD-deficient mutant cannot grow without extensive nutritional supplementation.) Physiological levels of NADH saturated the O_2^--generating activity, whereas normal levels of NAD^+ noncompetitively inhibited the activity by about 70%. The rate of cytosolic O_2^- production was normalized to the number of cells from which the extract was prepared in order to appraise its contribution to total intracellular O_2^- levels (see below). This is likely to overestimate its true value, since the normal electron acceptor is not present in the dialyzed extracts to compete with oxygen for the electrons of the NADH-reduced enzyme.

Other metabolites reduce redox-active enzymes that could in principle contribute to O_2^- production *in vivo*. For these contributions to be quantitatively significant with respect to

TABLE IV

Relative respiratory activities with various substrates

Cells were harvested during log-phase growth in the indicated media, membrane vesicles were prepared, and the substrate-specific respiratory activities were measured as described under "Materials and Methods." Values are normalized to the NADH-dependent respiratory activity for each vesicle preparation (≡). These values are representative; activities vary somewhat among different cell preparations. ND, not determined.

	LB + glucose	Minimal salts + glucose	Casamino acids
NADH	≡1.00	≡1.00	≡1.00
Succinate	0.01	0.09	1.51
D-Lactate	0.01[a]	0.02	0.11
L-Lactate	0.01[a]	0.01	0.16
α-Glycerophosphate	ND	0.07	0.73

[a] Assayed with D,L-lactate.

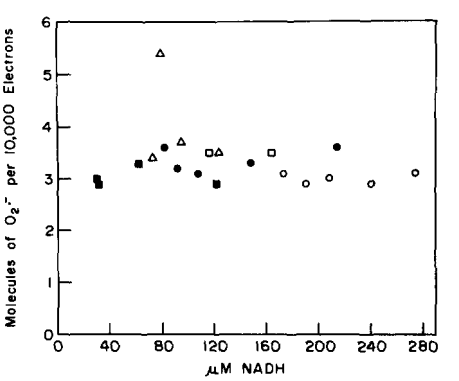

FIG. 3. **Fractional O_2^- production by the respiratory chain is independent of NADH concentration.** Median value = 3.25 molecules of O_2^-/10,000 electrons. Superoxide production and respiratory flux were determined with membrane vesicles from AB1157 with 2 mM NAD^+ as described under "Materials and Methods." Multiple experiments are indicated. □, 0.15 unit/ml NADH oxidase and 0.95% ethanol; ●, 0.15 unit/ml NADH oxidase and 1.9% ethanol; ○, 0.15 unit/ml NADH oxidase and 3.8% ethanol; △, 0.07 unit/ml NADH oxidase and 0.76% ethanol; ■, 0.09, 0.18, 0.35, and 0.36 unit/ml NADH oxidase (for 121, 62, 31, and 30 μM NADH, respectively) and 0.76% ethanol.

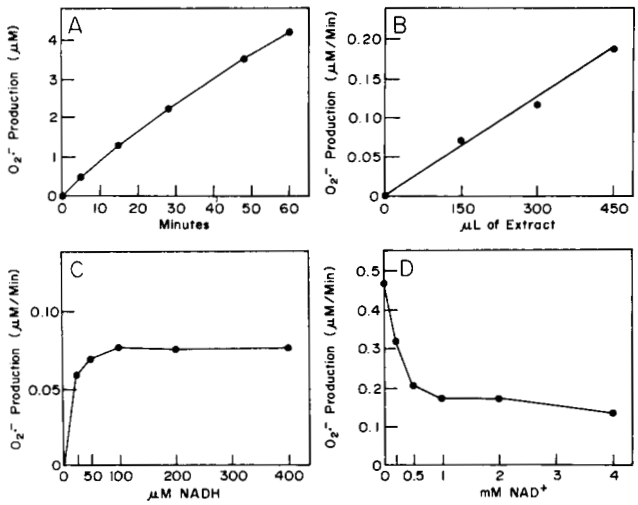

FIG. 4. **Superoxide production by NADH-treated dialyzed cytosol fraction at 37 °C.** *A*, time course of O_2^- production by 0.4 mg of extract. *B*, superoxide production *versus* volume of 1.9 mg protein/ml extract. *C*, dependence of O_2^- production by 0.4 mg of protein extract on NADH concentration. NAD^+ is 2 mM. *D*, dependence of O_2^- production by 0.4 mg of protein extract on NAD^+ concentration. NADH is 100 μM.

that of the respiratory chain, these enzymes would have to handle a very large electron flux and/or pass a large fraction of that flux to oxygen. No enzymes in *E. coli* are known to have O_2^- as a usual reaction product. O_2^- production was assayed in extracts incubated with the reductive substrates of the major carbon metabolic pathways. Glyceraldehyde 3-phosphate, L-lactate, pyruvate, isocitrate, α-ketoglutarate, malate, 6-phosphogluconate, and glucose 6-phosphate did not support significant generation of O_2^-. Succinate, which transfers electrons directly to the respiratory chain, did generate O_2^- in the presence of membrane vesicles; however, the activity of the succinate dehydrogenase, and thus the amount of O_2^-, is slight in glucose-grown cells. Therefore, the rate of cytosolic O_2^- measured *in vitro* with NADH should provide a reliable upper limit for that which pertains *in vivo*.

Calculation of O_2^- Production—Knowledge of the cell number, volume, respiration rate, and O_2^- production as a fraction of total respiration, allows calculation of the intracellular O_2^- flux from the respiratory pathway (Table V).

Log-phase cells cultured in LB with glucose consume $6.2 \cdot 10^6$ molecules of oxygen/s, maintain an intracellular solvent-accessible volume of $3.2 \cdot 10^{-15}$ liters/cell and make O_2^- at a frequency of about 3.25 molecules/10,000 electrons transferred (2500 molecules of O_2 reduced).

$$O_2^-/s = (3.25 \text{ molecules } O_2^-) \times (2500 \text{ molecules } O_2 \text{ consumed})^{-1}$$
$$\times (6.2 \cdot 10^6 \text{ molecules } O_2/s) = 8100 \text{ molecules/s/cell}$$

Division by Avogadro's number and by the intracellular volume reveals that O_2^- is made by the respiratory system at a rate of 4.2 μM/s. Similar calculations for cells grown on minimal medium produce values of 1200 molecules O_2^-/cell/s and 2.9 μM O_2^-/s.

The contribution of the cytosolic enzymes to intracellular O_2^- can be estimated from the O_2^- formation by the soluble lysate fraction during incubation with NAD(P)H. For the reasons discussed above, the value obtained is likely to be an overestimate. Assays at 37 °C of three independent cell preparations produced values of 2800, 3400, and 2700 molecules of O_2^-/s/cell (1.5 μM/s). These compare to 8100 molecules/s/cell of membrane-generated O_2^-. Thus, even if these values of cytosolic O_2^- production are not treated as overestimates,

TABLE V

Superoxide production rates and steady-state levels in log-phase E. coli

See text for calculations. Steady-state O_2^- levels have been calculated for SOD-proficient cells in which enzymatic dismutation is the route of O_2^- elimination. Levels have also been predicted for SOD-deficient cells in the cases in which reaction with either glutathione or spontaneous dismutation is considered the major route of O_2^- elimination. ND, not determined.

	O_2^- production	
	LB	Minimal salts
	μM/s	
Respiratory	4.2	2.9
Cytosolic	1.5	ND
Sum	5.7	≥2.9
	Steady-state O_2^-	
	LB	Minimal salts[a]
	M	
Accumulation limited by:		
SOD	$2.0 \cdot 10^{-10}$	$1.5 \cdot 10^{-10}$
Glutathione	$4.9 \cdot 10^{-7}$	$2.5 \cdot 10^{-7}$
Spontaneous dismutation	$6.7 \cdot 10^{-6}$	$4.8 \cdot 10^{-6}$

[a] Because the cytosolic contribution to O_2^- production is unknown and expected to be minor, it has been disregarded in these calculations.

about 75% of the intracellular O_2^- is due to electron leakage from the respiratory chain.

Steady-state O_2^- Levels in Growing Cells—The O_2^- production rates and intracellular SOD activities can be combined to determine the steady-state concentration of O_2^- within the cells (Table V). Cells cultured in LB + glucose contain about 3600 units/ml of SOD activity. Since a unit of SOD is defined as the amount of enzyme that inhibits by 50% the reduction of 3 ml of 10 μM ferricytochrome *c* (k_{cyc} with $O_2^- = 2.6 \times 10^5$ M^{-1} s^{-1} (25)), the pseudofirst-order rate constant of 1 unit/ml SOD with O_2^- is 7.8 s^{-1}.

The rate of production is the sum of the rates by respiratory and cytosolic sources, 4.2 and 1.5 μM/s, respectively.

$$\text{Rate of } O_2^- \text{ production} = \text{rate of dismutation}$$

$$5.7 \text{ μM/s} = 3600 \text{ units/ml SOD} \times 7.8 \text{ s}^{-1}(1 \text{ unit/ml SOD})^{-1} \times [O_2^-]$$

At the steady state, internal $O_2^- = 2.0 \cdot 10^{-10}$ M. If the questionable contribution of cytosolic O_2^- sources is omitted, the calculated O_2^- concentration in LB-grown cells is $1.5 \cdot 10^{-10}$ M. Similar calculations for cells grown in minimal medium, where both respiratory O_2^- fluxes and SOD activities are somewhat lower, also arrive at a steady-state O_2^- concentration of $1.5 \cdot 10^{-10}$ M.

Because superoxide dismutes spontaneously, one might wonder about the necessity of having an enzyme to catalyze what is already a fast reaction. The importance of SOD can be understood by calculating the steady-state level that would result if the intracellular lifetime of superoxide were limited by its spontaneous rather than enzymatic dismutation. At neutral pH the spontaneous dismutation is due to the following reaction.

$$HO_2^\cdot + O_2^- \rightarrow H_2O_2 + O_2, \; k = 8 \times 10^7 \text{ M}^{-1} \text{ s}^{-1}$$

The pK_a of superoxide is 4.8 (26), so at the intracellular pH of ~7.6, $[HO_2^\cdot] = 1.58 \cdot 10^{-3} [O_2^-]$. Thus, 5.7 μM/s = $k[HO_2^\cdot] \times [O_2^-] = (8 \cdot 10^7 \text{ M}^{-1} \text{ s}^{-1})(1.58 \cdot 10^{-3}) [O_2^-]^2$ and the steady-state concentrations of O_2^- would be $6.7 \cdot 10^{-6}$ M, over 30,000 times the level obtained in SOD-proficient cells. In the small volume of a single cell that is generating 11,000 molecules of O_2^-/s,

the steady-state level of $2 \cdot 10^{-10}$ M equates to a time-average of only 0.4 molecules of O_2^-/cell and $6.7 \cdot 10^{-6}$ M, to 13,000 molecules/cell. The advantage of enzymatic catalysis is profound.

O_2^- Gradient from Membrane into Cytosol—Because most of the O_2^- is generated on the inside surface of the membrane, the local steady-state concentration will be higher there than in the cytosol. As a consequence membrane constituents will be subjected to greater oxidative stress than will cytosolic biomolecules. The severity of this gradient can be calculated by modelling O_2^- diffusion from an idealized cell membrane. If the cell is construed as a cylinder of radius R and length L, the internal volume is given by $v = \pi R^2 L$. The relation of radius to cell length has been reported variously as $L/2R$ = 2.75, 3.46, and 4.73 for cells growing quickly in rich medium (27); the disparities are due to variations in the method of measurement. If the intermediate value is selected, R is 0.53 μm and L is 3.7 μm for a cell of the internal volume $3.2 \cdot 10^{-15}$ liters. If the first-order rate constant for superoxide consumption by the intracellular SOD is k, D is the diffusion constant, t is time, and C is the O_2^- concentration, then at any distance r from the center of the cell, the superoxide concentration is related to diffusion and dismutation by the following equation.

$$\frac{\partial C}{\partial t} = D\left[\frac{\partial^2 C}{\partial r^2} + \frac{1}{r}\frac{\partial C}{\partial r}\right] - kC$$

At the steady-state, $\frac{\partial C}{\partial t} = 0$. The solution of this equation is

$$C = \frac{F_0}{\sqrt{kD}}\left[\frac{I_0\left(\sqrt{\frac{k}{D}}\right) r}{I_1\left(\sqrt{\frac{k}{D}}\right) R}\right]$$

where F_0 is the rate of O_2^- production per unit membrane area and I_0 and I_1 are hyperbolic Bessel functions. The membrane area, excluding end effects, is $2\pi R \cdot L = 1.2 \cdot 10^{-7}$ cm^2. F_0 is then $1.2 \cdot 10^{-13}$ mol/cm^2/s. In cells containing normal SOD activity, $k = 27{,}800$ s^{-1}. For a small molecule, D will be about 10^{-5} cm^2 s^{-1}. The steady-state O_2^- concentration is presented as a function of the distance from the cell membrane in Fig. 5. In this model, where only membrane-generated O_2^- is considered, a 4-fold decline of O_2^- occurs from the cell membrane to the cell center. If cytosolic biomolecules are assumed to each exist at random distances from the membrane, their average O_2^- exposure is the total intracellular O_2^- concentration, $1.5 \cdot 10^{-10}$ M. The O_2^- concentration at the cell membrane is somewhat higher, $2.6 \cdot 10^{-10}$ M. (Inclusion of the possible cytosolic contribution to O_2^- production increases both values slightly, to $2.0 \cdot 10^{-10}$ M and $3.1 \cdot 10^{-10}$ M, and moderates the gradient somewhat.) Thus at basal SOD levels the superoxide exposure does not vary greatly between cytoplasmic and membrane-bound biomolecules. However, at the 7-fold higher SOD levels that are achieved by enzyme induction (28), the gradient becomes steeper as the mean lifetime and diffusion distance of the superoxide molecules declines (Fig. 5).

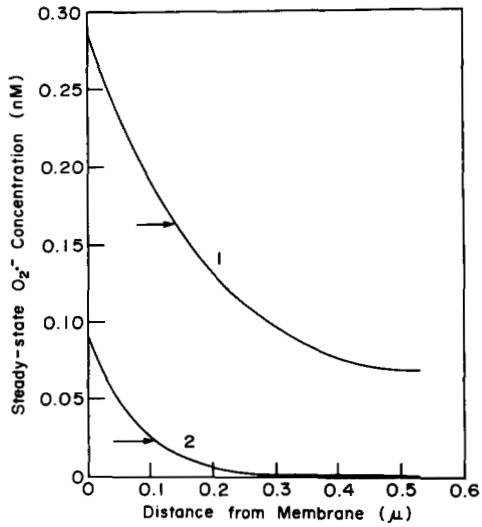

FIG. 5. **Calculated superoxide gradient from the cell membrane to the cell center.** The cell radius is 0.53 μm. See text for calculation. Calculations assume no cytosolic O_2^- source. *Curve 1*, SOD concentration is that of log-phase cells grown in aerobic rich medium. The ratio of steady-state O_2^- at the membranes to the average cytosolic concentration is 1.74. *Curve 2*, SOD is induced 7-fold above the basal level. O_2^- ratio (membrane/cytosol) is 3.85. *Arrows*, mean intracellular O_2^- concentration. Seven-fold SOD induction lowers the cytosolic O_2^- level 7-fold but the membrane exposure only 3.2-fold.

DISCUSSION

Metabolic O_2^- production in growing *E. coli* is due primarily to leakage of electrons from the respiratory chain. Most or all of this leakage occurs from the respiratory dehydrogenases.[2] Since virtually all respiration in glucose-grown cells is NADH-dependent, *in vitro* measurement of O_2^- production as a fraction of NADH-dependent oxygen consumption allows an estimate of O_2^- production rates in whole cells. The existence of *E. coli* strains devoid of SOD activity has permitted a search for superoxide-generating enzymes in the soluble fraction. Although the survey of reductive substrates for cytosolic enzymes cannot be considered definitive, none was capable of approaching the O_2^--generating capacity of respiratory substrates, and few or no untested metabolites are likely to be processed at a flux great enough to make much superoxide, even if the efficiency were significantly higher than that during the oxidation of respiratory substrates. This result is not surprising; few metabolic pathways can match the pace of electron transfer by the membrane-associated respiratory chain, and unlike the respiratory pathways, most cytosolic redox enzymes carry out the concerted transfer of a pair of electrons and are expected not to be prone to univalent autoxidation. Massey and colleagues (29) have observed the tendency of reduced flavoenzymes to generate O_2^-, due to the stability of the flavosemiquinone product. Respiratory dehydrogenases are all flavoproteins, whereas relatively few redox-active cytosolic enzymes are. Among the enzymes of the central carbon metabolic pathways, which would experience a substrate flux comparable to that of the respiratory pathway, only the pyruvate, α-ketoglutarate, and succinate dehydrogenases are known to contain flavins. All of these enzymes are repressed during growth on glucose and failed to generate significant O_2^- in the extracts of glucose-fed cells.

O_2^- production by NAD(P)H-treated cytosol appears to be due to a single enzyme. Glutathione reductase is a prominent soluble flavoenzyme that can accept either NADH or NADPH as a reductant, and the yeast enzyme has been shown to make O_2^- (29). This enzyme may be the cytosolic O_2^- generator in *E. coli*.

Other methods designed to measure O_2^- production are not applicable to *E. coli*. The detection limit for O_2^- of the spin trap DMPO has been estimated to be 10^{-8} M; thus, its failure to trap measurable O_2^- in *E. coli* is not surprising (30). Cyanide-resistant respiration has also been used as a measure of O_2^- production by mitochondria (31) and by *E. coli* during

[2] J. Imlay and I. Fridovich, unpublished data.

treatment with redox-cycling agents (32). However, the K_I values for cyanide of the major and minor cytochrome oxidases of *E. coli* are 10 μM and 2 mM, respectively; since basal superoxide production represents only about 0.1% of the total respiration, an extremely high concentration of cyanide would be necessary to reduce the background of cyanide-sensitive respiration sufficiently to allow detection of the cyanide-resistant fraction. The utility of the method is restricted to experiments with *E. coli* in which redox-active compounds, such as viologens and quinones, elevate O_2^- formation to >5% of the total oxygen consumption.

Tyler (12) estimated O_2^- levels in isolated rat liver mitochondria by measuring mitochondrial SOD activity and using the H_2O_2 production rates that were measured by Boveris *et al.* (33), and his estimated steady-state value of $8 \cdot 10^{-12}$ M has been widely cited. Tyler (12) regarded this number as an upper limit, since it was derived from the O_2^- production rates of succinate-fed state-four mitochondria, when O_2^- generation was maximal; other respiratory substrates produced significantly less O_2^-, and the addition of ADP reduced the rate by about an order of magnitude. Additionally, physiological O_2^- levels are likely to be further reduced, since the dissolved oxygen concentration is low in animal tissues. H_2O_2 generation rates were also determined for non-mitochondrial fractions (33), but the majority of this H_2O_2 is probably a direct product of various oxidases rather than the result of O_2^- dismutation, and as such cannot be used to calculate non-mitochondrial O_2^- levels.

Mitochondrial O_2^- production accounts for 2–4% of total oxygen consumption, whereas the figure is ~0.1% in *E. coli*. The disparity in leakiness reflects the considerable differences in electron-chain organization. Total O_2^- production is much greater in *E. coli* only because of the phenomenal rate of respiration in this bacterium. In fact, a vigorous facultative aerobe such as *E. coli* might not be able to tolerate the relatively leaky electron-transport structure of mitochondria, since the attendant O_2^- production would result in extreme oxidative stress.

It is of interest to determine the steady-state levels of O_2^- that are sufficient to disable various cell functions. SOD-deficient strains fail to synthesize various amino acids, mutate rapidly, and have a slow-growth phenotype indicative of additional unknown dysfunctions. The calculation above of a steady-state O_2^- level that would be achieved if spontaneous dismutation were the sole route of O_2^- dissipation ($7 \cdot 10^{-6}$ M) represents an upper limit for the SOD mutants, since it is likely that O_2^- is consumed by other reactions and accumulates to a far lower level. For example, reduced glutathione, which is present at 4–5 mM in these cells (data not shown), scavenges O_2^- at a rate of $2.6 \cdot 10^3$ M^{-1} s^{-1} (derived from Ref. 34) and would restrict O_2^- accumulation to $5 \cdot 10^{-7}$ M. Glutathione may not be the predominant co-reactant with O_2^-, and it is not depleted in SOD-deficient mutants (data not shown). Knowledge of the identity and rate of the primary O_2^--scavenging reaction in SOD mutants will allow calculation of the O_2^- concentration that results in the severe phenotypic deficiencies of these mutants.

Dissection of superoxide-sensitive pathways in *E. coli* will allow further identification of enzymes that are inactivated by O_2^-. Measurements of the inactivation rates *in vitro* permits estimation of their inactivity status in oxidatively stressed cells. For example, the 6-phosphogluconate dehydratase of *E. coli* exhibits an activation rate with O_2^- in excess of $1 \cdot 10^8$ M^{-1} s^{-1} (11). Amazingly, in SOD-proficient cells ($2 \cdot 10^{-10}$ M O_2^-), the half-life of this enzyme activity would be only 40 s; in the SOD-deficient strain (using $O_2^- = 5 \cdot 10^{-7}$ M), one-hundredth of a second. Gardner and Fridovich (11) detected low activity (<10% of wild-type levels) in the extract of an SOD mutant, which suggests that cells must have some process to repair the superoxide-inactivated active-site iron-sulfur cluster. Such a process was observed in studies of another O_2^--sensitive dehydratase, dihydroxyacid dehydratase, during anaerobic incubation of crude extracts (9). Presumably the balance between superoxide levels and the reactivation rate determines whether the enzyme is functional.

The direct agent of hyperbaric oxygen toxicity may be O_2^-. Indeed, superoxide-generating drugs and hyperoxia cause the failure of many of the same biosynthetic enzymes in *E. coli* (35). This hypothesis may be tested by a comparison of the steady-state O_2^- levels induced by disabling doses of redox-cycling drug and of hyperoxia. The production rates of O_2^- in hyperbaric oxygen can be extrapolated from the data of this study, since no significant oxygen gradient exists over the cell membrane and since O_2^- production should increase linearly with the oxygen concentration. Basal superoxide fluxes have been determined here with the extracts of cells grown on both minimal and rich media, so that either medium might be used in characterizing responses to oxidative stress.

Researchers have long known that the imposition of oxidative stress, administered by γ-radiation, peroxides, hyperbaric oxygen, or redox-cycling drugs, can cause growth abnormalities, stasis, and death. The suspicion that the oxidative agents that enforce those effects are trace by-products of normal cell metabolism has engendered theories that link disease states to cumulative oxidative cell damage. The connection between the observed consequences of imposed stress and the postulated consequences of endogenous stress cannot be confirmed until the quantitative relationship is determined.

Acknowledgments—We thank Dr. Jacob J. Blum for his invaluable assistance in calculating the superoxide gradient.

REFERENCES

1. Naqui, A., Chance, B., and Cadenas, E. (1986) *Annu. Rev. Biochem.* **55,** 137–166
2. Bilinski, T., Krawiec, Z., Liczmanski, A., and Litwinska, J. (1985) *Biochem. Biophys. Res. Commun.* **130,** 533–539
3. van Loon, A. P. G. M., Pesold-Hurt, B., and Schatz, G. (1986) *Proc. Natl. Acad. Sci. U. S. A.* **83,** 3820–3824
4. Carlioz, A., and Touati, D. (1986) *EMBO J.* **5,** 623–630
5. Phillips, J. P., Campbell, S. D., Michaud, D., Charbonneau, M., and Hilliker, A. J. (1989) *Proc. Natl. Acad. Sci. U. S. A.* **86,** 2761–2765
6. Farmer, K. J., and Sohal, R. S. (1989) *Free Rad. Biol. Med.* **7,** 23–29
7. Adelman, R., Saul, R. L., and Ames, B. N. (1988) *Proc. Natl. Acad. Sci. U. S. A.* **85,** 2706–2708
8. Farr, S. B., D'Ari, R., and Touati, D. (1986) *Proc. Natl. Acad. Sci. U. S. A.* **83,** 8268–8272
9. Kuo, C. F., Mashino, T., and Fridovich, I. (1987) *J. Biol. Chem.* **262,** 4724–4727
10. Flint, D. H., and Emptage, M. H. (1990) in *Biosynthesis of Branched-chain Amino Acids* (Barak, Z., Chipman, D., and Schloss, J. V., eds) pp. 285–314, V. C. H. Weinheim/Deerfield Borch and Balaban, Rehovoth/Philadelphia
11. Gardner, P., and Fridovich, I. (1991) *J. Biol. Chem.* **266,** 1478–1483
12. Tyler, D. D. (1975) *Biochem. J.* **147,** 493–504
13. Imlay, J. A., and Linn, S. (1987) *J. Bacteriol.* **169,** 2967–2976
14. Young, I. G., and Wallace, B. (1976) *Biochim. Biophys. Acta* **449,** 376–385
15. Miller, J. H. (1972) Experiments in Molecular Genetics, pp. 431–432, Cold Spring Harbor Laboratory, Cold Spring Harbor, NY
16. Rosen, B. P., and McClees, J. S. (1974) *Proc. Natl. Acad. Sci. U. S. A.* **71,** 5042–5046
17. Bradford, M. M. (1976) *Anal. Biochem.* **72,** 248–254

18. McCord, J. M., and Fridovich, I. (1969) *J. Biol. Chem.* **244,** 6049–6055
19. Lundquist, R., and Olivera, B. M. (1971) *J. Biol. Chem.* **246,** 1107–1116
20. Karp, M. T., Raunio, R. P., and Lovgren, T. N-E. (1983) *Anal. Biochem.* **128,** 175–180
21. Leder, I. G. (1972) *J. Bacteriol.* **111,** 211–219
22. Boveris, A., and Chance, B. (1973) *Biochem. J.* **134,** 707–716
23. Boveris, A., and Cadenas, E. (1982) in *Superoxide Dismutase* (Oberley, L. W., ed) Vol. 2, p. 25, CRC Press, Boca Raton, FL
24. Kita, K., Konishi, K., and Anraku, Y. (1984) *J. Biol. Chem.* **259,** 3375–3381
24a Neidhardt, F. C. (1987) in *Escherichia coli and Salmonella typhimurium* (Neidhardt, F. C., ed) Vol. 1, p. 4, American Society of Microbiology, Washington, D. C.
25. Fridovich, I. (1985) in Handbook of Methods for Oxygen Radical Research (Greenwald, R. A., ed) pp. 51–53, CRC Press, Boca Raton, FL
26. Fridovich, I. (1978) *Science* **201,** 875–880
27. Cooper, S. (1989) *J. Bacteriol.* **171,** 5239–5243
28. Pugh, S. Y. R., DiGuiseppi, J. L., and Fridovich, I. (1984) *J. Bacteriol.* **160,** 137–142
29. Massey, V., Strickland, S., Mayhew, S. G., Howell, L. G., Engel, P. C., Matthews, R. G., Schuman, M., and Sullivan, P. A. (1969) *Biochem. Biophys. Res. Commun.* **36,** 891–897
30. Schellhorn, H. E., Pou, S., Moody, C., and Hassan, H. M. (1989) *Arch. Biochem. Biophys.* **271,** 323–331
31. Freeman, B. A., Crapo, J. D. (1981) *J. Biol. Chem.* **256,** 10986–10992
32. Hassan, H. M., and Fridovich, I. (1979) *Arch. Biochem. Biophys.* **196,** 385–395
33. Boveris, A., Oshino, N., and Chance, B. (1972) *Biochem. J.* **128,** 617–630
34. Wefers, H., and Sies, H. (1983) *Eur. J. Biochem.* **137,** 29–36
35. Brown, O. R., and Seither, R. L. (1983) *Fundam. Appl. Toxicol.* **3,** 209–214